Applied Radiation and Isotopes 160 (2020) 109082

Contents lists available at ScienceDirect

Applied Radiation and Isotopes

journal homepage: http://www.elsevier.com/locate/apradiso

Correction factors for non-uniform large-area reference sources

Iremar Alves Silva Jr. [a,b,*], Paulo de T.D. Siqueira [a], Eduardo do Nascimento [c], Hélio Yoriyaz [a], Gian-Maria A.A. Sordi [a], Vitor Vivolo [a], Maria da Penha A. Potiens [a]

[a] Instituto de Pesquisas Energéticas e Nucleares, São Paulo, SP, CEP:05508-000, Brazil
[b] Universidade de São Paulo - Butantã, São Paulo, SP, CEP:05508-000, Brazil
[c] Universidade Federal da Bahia - Ondina, Salvador, BA, CEP:40170-115, Brazil

ARTICLE INFO

Keywords:
Correction factors
Uniformity
Non-uniform
Instrument efficiencies
Large-area reference sources

ABSTRACT

Based on uniformity measurements of large-area reference sources used in calibration procedures of surface contamination monitors, an investigation was carried out to obtain a method that estimates the bias originated from surface source intensity distribution deviation from the ideal uniform distribution and corrects it. It relies on correcting the estimated instrument efficiency by applying correction factors driven from the uniformity distribution profiles of the sources used in calibration procedure. Simulations of the monitor calibration procedure are run for 2 distinct surface source distributions: the real and the ideally uniform distributions. Correction factors are driven from counting rate estimates obtained from each source representation. In order to evaluate adequacy of this proposition it was validated against a method proposed by the NPL in the Good Practices Guide No.14.

1. Introduction

ISO 7503-3:2016 (ISO, 2016), one of the main documents for the calibration of surface contamination monitors states that radiation monitors should have their responses tested satisfactorily for each specific type of ionization radiation (alpha, beta and photon). ISO 8769:2016 (ISO, 2016), in its turn, specifies the main characteristics of the large-area reference sources (LARS) that should be used in the operational tests and in the calibration of surface contamination monitors. This document recommends that these sources should be traced by national or international measurement standards, be flat and have a uniformity value greater than 90%. Source uniformity has deserved some attention for some time as can be observed by recommendations addressed by ISO 8769:2016. It not only recommends the surface emission mapping as one of the inherent information of new LARS but also suggests the experimental mapping procedure to evaluate source uniformity. This marked concern on setting these procedures might be explained by the fact that instrument calibration methodology relies on the 100% uniformity value of the LARS. Any deviation from uniformity shall therefore impose a bias on the instrument efficiency estimates. However producing a uniform LARS is practically unfeasible in a thorough way. Besides, there are studies in the literature that report differences between the uniformity values of the LARS used in the calibration of surface contamination monitors (Vivolo and Potiens, 2010; Silva Junior et al., 2014; Ohshiro et al., 2016) and the requirements of ISO 8769:2016. This work presents a methodology to estimate the bias on the evaluation of the instrument efficiency brought about by source non-uniformity and also provides a correction factor that may be used to remove this bias. Instrument efficiency is evaluated by simulating the instrument calibration set up under two different surface source intensity distributions: the ideal uniform distribution and the actual surface source distribution. Correction factors are driven from the instrument counting efficiency simulated results. The use of correction factors to deal with the uniformity, or the absence of ideal uniformity, is not a novelty by itself, as it has already been proposed before by NPL in the Good Practices Guide No. 14 (Lee et al., 2014). This work presents an alternative calculation methodology, based on the Monte Carlo code, MCNP5 (X-5 Monte Carlo Team,i, 2003), which provides correction factors to be incorporated in the instrument calibration procedures using large-area reference sources, enabling more accurate instrument efficiency evaluation. A comparison between both methodologies shows a good agreement between the retrieved results. This comparison is presented along this work.

* Corresponding author. Instituto de Pesquisas Energéticas e Nucleares, São Paulo, SP, CEP:05508-000, Brazil.
E-mail address: iremarjr@alumni.usp.br (I.A. Silva).

https://doi.org/10.1016/j.apradiso.2020.109082
Received 7 October 2019; Received in revised form 11 February 2020; Accepted 12 February 2020
Available online 24 February 2020

Table 1
Large-area reference source certified data.

Nuclide Source	Source Number	R_c ($\beta.s^{-1}$)
^{14}C	FG498	405 ±10
^{99}Tc	FG773	572 ±15
^{36}Cl	FI215	643 ±16
^{90}Sr FG499	849 ±22	

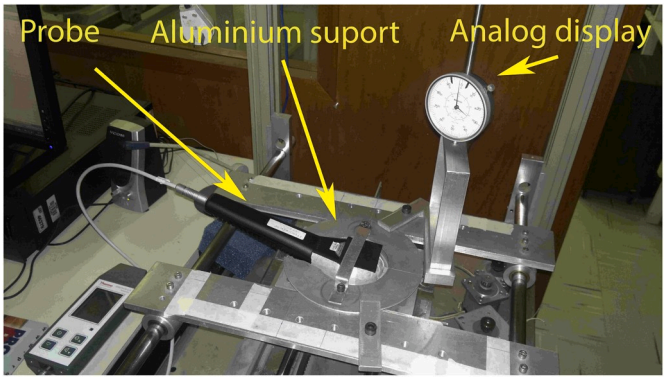

Fig. 1. Experimental calibration set-up.

2. Materials and methods

Measurements were done by using 10.0 cm × 15.0 cm, ^{14}C, ^{99}Tc, ^{36}Cl and ^{90}Sr, large-area reference sources at the Instrument Calibration Laboratory in the Institute of Energy and Nuclear Research (LCI-IPEN). These large-area reference sources were produced by Amershan, and their certified data, from the DKD (*DeutscherKalibrierdienst*) are shown in Table 1. It includes the radionuclide emitter, its identification number and its corrected beta surface emission rate (R_c) to the time when the experiments were run. Measurements were performed using a Thermo radiation monitor model FH 40 GX and a pancake type probe model FHZ 732 GM, which has a sensitive area of 15.5 cm^2 , as recommended by the Good Practice Guide No.14.

2.1. Source intensity distribution mapping

The uniformity mapping procedure of the large-area reference sources consisted in dividing each of the sources into 24 independent regions (cells), each cell measuring 2.5 cm × 2.5 cm (6.25 cm^2). These cells were distributed along an array of four rows and six columns. To carry out the measurement of the activity fraction for each of these cells, counting rate measurements were performed using a 0.2 cm thick aluminum mask, with a central square aperture with the same dimensions of each cell. This mask was positioned over the large-area reference source, restricting the passage of radiation from one cell at a time, shielding the probe from the emissions of the other 23 cells. To assist in this procedure 24 paper templates with the same size of the source were made. Each of these templates contains specific mold corresponding to each cell of the source to be measured according to its size. Adjusting the aluminum mask over the mold of the template facilitated the correct positioning of the aluminum mask. Then, the pancake probe was positioned over the aperture in the mask in order to limit the counting rate measurement contribution mostly to radiation emerging from the selected cell. This procedure was repeated for each cell of the source using the specific paper template.

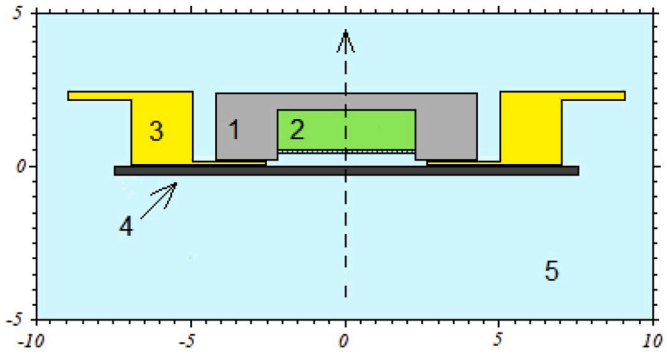

Fig. 2. Simulated arrangement cross section geometry.

2.2. Calibration system

The monitor calibration set up used consists of an aluminum support, with a central circular aperture, which holds the monitor probe under calibration and places it exactly over the center of the large-area reference source with a distance of 3 mm between them (Fig. 1).

The calibration procedure consisted on ten counting rate measurements. The instrument efficiency (ε) was calculated by the ratio of the observed net counting rate (ρ_c), i.e., the total minus background counting rates, and the source emission rate below the probe area (SER) as shown in equation (1).

$$\varepsilon = \frac{\rho_c}{SER} \tag{1}$$

SER, was obtained from the data provided by the source calibration certificate and the probe size, according to equation (2).

$$SER = \left(\frac{R_c}{S_c} \times S_p\right) \tag{2}$$

R_c is the large-area reference source surface emission rate corrected for the day of calibration procedure; S_c is the active area of the large-area reference source; and S_p is the sensitive area of the probe.

2.3. Monte Carlo simulation

MCNP5 is a Monte Carlo based radiation transport code that can simulate coupled photon and electron transport for general configuration system and purposes. It was chosen as a calculation tool not only for the available simulation resources, but also for being a widely validated radiation transport code and corroborated in the evaluation of parameters of the most different systems, particularly in the assessment of detection efficiency of most diverse detectors and in the representation of different radiation sources (Ródenas et al., 2005; Farsoni and Hamby, 2005; Choi et al., 2016; Grujić et al., 2013).

Fig. 2 shows the schematic cross section view of the calibration system modeling used in the MCNP5 simulations. It consists of a cylindrical radiation probe, made of a stainless steel structure (1) embracing the cylindrical active gaseous volume (2). A thin mica sheet, protected by a reticular stainless steel grid, makes up the radiation entrance window. The probe was placed on the probe support (3) at the center of its circular aperture in such a way to preserve the cylindrical symmetry. The large-area reference source (4) was represented by an aluminum board placed under the probe support and centered along the symmetry axis. The whole setup was immersed in air (5). The self-absorption and backscattering were considered by taking into account the particle interaction with the aluminum board and with air around the set.

Beta emission energy spectra were obtained from RADAR (RADAR) and the $^{90}Sr + {}^{90}Y$ spectrum was obtained by a combination of the spectrum of each element.

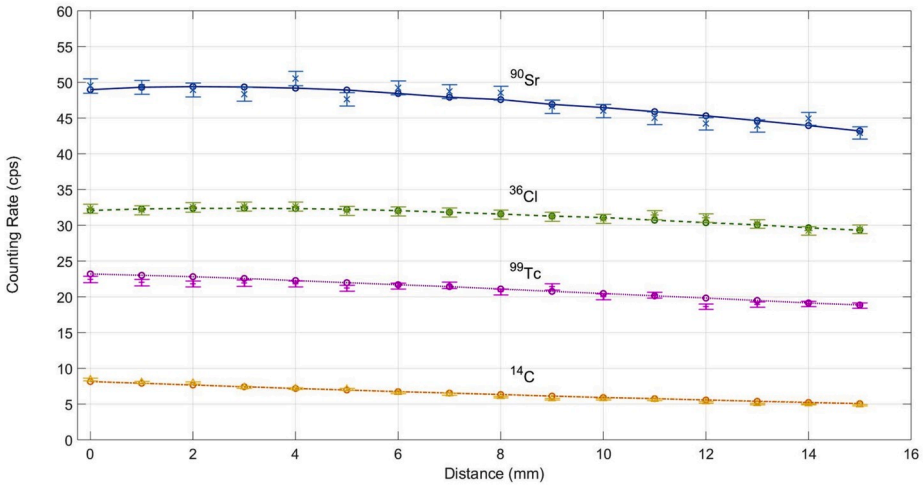

Fig. 3. Experimental and simulated detector counting rates dependence on source to detector distance for the four large-area reference sources used in the present work.

2.4. Validation

Validation experiments were performed in order to get confidence on the simulation results and on their use through the work. The experiments consisted on recording the probe counting rate for a series of source-detector distances. Source-detector setup distance was changed from 0 to 15 mm at 1 mm steps for each one of the four large-area reference source used. Simulations were run for each of the experimental arrangement using the measured source distribution intensity distribution (non-uniform). Fig. 3 shows the experimental and simulated counting rate results. Simulated values are represented by circles joined by lines that stand as visual guides. Experimental values are represented by signs and a ± one standard deviation bar. Uncertainties on the beta surface emission rates (2.5% for one standard deviation confidence level) have not been propagated to the simulation results shown in the figure so to stress the statistical precision of simulated results (below 0.2%). The uncertainties on the experimental data have been estimated as 2% and are shown in the figure. The largest absolute difference was found for the ^{90}Sr large-area reference source for 4 mm source detector distance, where the simulated result overestimated the experimental detector counting rate by 2.5 cps. This difference represents 5% of the calculated value, which is easily justified by the uncertainties on the experimental results and on the certified surface source emission rate.

These results have provided the confidence on the simulations carried on by showing that the main characteristics of the systems under study, i.e. the large-area reference sources and detector, have been successfully attained. Simulation results have therefore been used as the reference values to study the lack of the uniformity found on the actual large-area reference sources and to propose the correction factors methodology.

2.5. Correction factor

To obtain the correction factors two simulations were run for each source. These simulations differed from each other by their source intensity distributions. The source intensity distribution for each of the four sources was considered in two different representations: (1) 100% uniformity value source intensity distribution (uniform) and (2) Measured source intensity distribution (non-uniform). From the difference between the values obtained by the simulations for the two representations of the large-area reference source (uniform and non-uniform) it is possible to estimate a correction factor of the large-area reference source, providing a more accurate estimation for the instrument efficiency. The correction factor CF_{MCNP} is obtained by the ratio between the simulated counting rates for the uniform (ρ_u) and non-uniform (ρ_{nu}), representations, according to equation (3).

$$CF_{MCNP} = \frac{\rho_u}{\rho_{nu}} \tag{3}$$

The obtained correction factor CF_{MCNP} can be multiplied by the net counting rate measured by the probe (ρ_c), to get the corrected counting rate (ρ_{corr}), according to equation (4).

$$\rho_{corr} = \rho_c \times CF_{MCNP} \tag{4}$$

The corrected instrument efficiency using this methodology (ε_{MCNP}) is calculated as in equation (1), using the corrected counting rate (ρ_{corr}), as in equation (5).

$$\varepsilon_{MCNP} = \frac{\rho_{corr}}{SER} \tag{5}$$

It can also be calculated by applying equation (6).

$$\varepsilon_{MCNP} = \varepsilon \times CF_{MCNP} \tag{6}$$

2.6. NPL numerical method

The Good Practice Guide No.14 of the NPL also presents the proposition to adopt a uniformity correction procedure when using large-area reference sources in calibration procedures. However, the proposed numerical method is restricted to the increment of exactitude associated with the use of large-area reference sources with uniformity greater than 90%. The correction methodology presented by the guide corrects the surface emission rate of the large-area reference source, evaluating the instrument efficiency by equation (7).

$$\varepsilon = \frac{\rho_c}{SER_{eff}} \tag{7}$$

SER_{eff} is the effective surface emission rate per unit area under the probe and is given by equation (8).

$$SER_{eff} = \frac{\sum_i E_i . fi}{\sum_i fi} \; . \; SER \tag{8}$$

Where i is the set of cells that are totally or partially under the probe sensitive area; E_i is the relative activity of cell i, i.e., the ratio between the activity of cell i and the average activity value of all 24 cells obtained in the source activity distribution measurement and f_i is the fraction of the cell that is covered by the probe sensitive area.

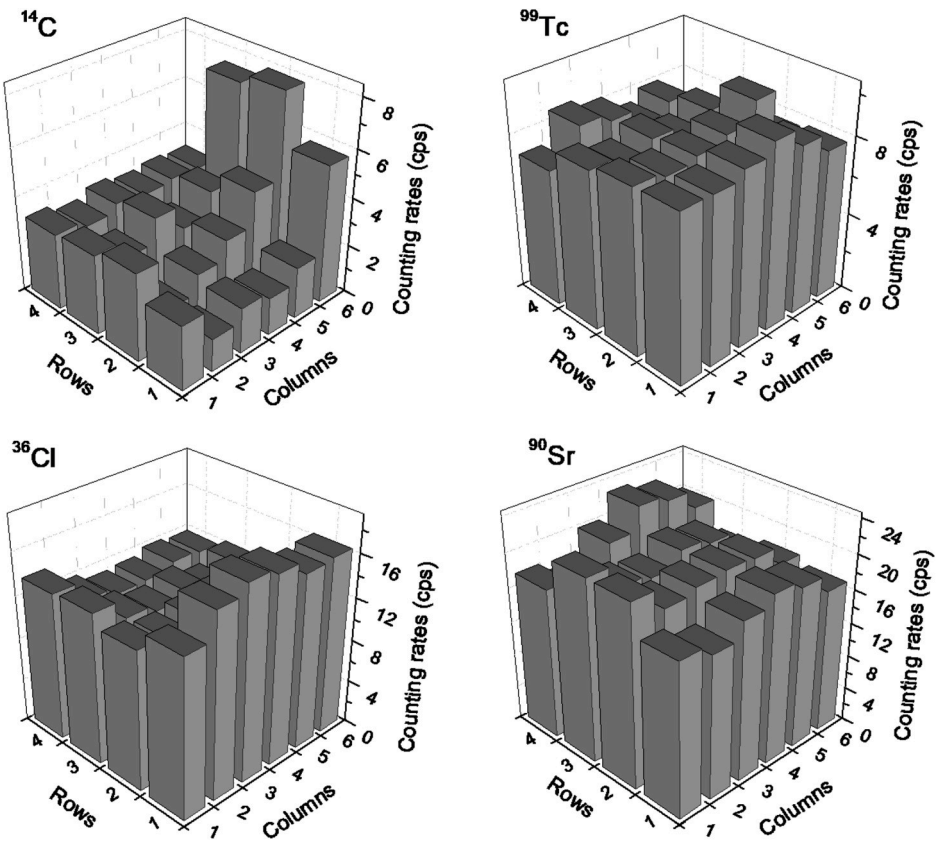

Fig. 4. Measured large-area reference source intensity distributions.

Table 2
Experimental source uniformity data.

Nuclide Source	Uniformity (%)	Relative Standard Uncertainty (%)
^{14}C	50.20	0.40
^{99}Tc	90.66	0.04
^{36}Cl	84.44	0.05
^{90}Sr	91.18	0.02

3. Results

3.1. Source mapping

Fig. 4 shows the surface source intensity distributions measured along the active area for each one of the four large-area reference sources used in this work, according to the procedures described in section 2.1.

Table 2 shows the uniformity values of the sources obtained from the sources intensity distributions. It shows that, only the ^{99}Tc and ^{90}Sr LARS meet the ISO 8769 uniformity criterion that recommends a 90% minimum value. Both sources present uniformity values close to the suggested minimum value while ^{14}C and ^{36}Cl, do not meet the ISO uniformity criterion, standing the ^{14}C far below the minimum value. The analysis of these sources will however be kept on along the work as an indication of the impact of LARS non uniformity on surface contamination detector efficiency inferred by calibration procedures had they been used.

Table 3
Counting rates (ρ_c), source emission rates (SER) and evaluated efficiencies obtained by the standard calibration procedure (ε).

Nuclide Source	ρ_c (cps)	SER ($\beta.s^{-1}$)	ε (%)
^{14}C	8.46 ±0.16	41.9 ±1.0	20.2 ±0.6
^{99}Tc	22.43 ±0.25	59.1 ±1.6	38.0 ±1.1
^{36}Cl	32.35 ±0.30	66.4 ±1.7	48.7 ±1.3
^{90}Sr	49.53 ±0.30	87.7 ±2.3	56.5 ±1.5

Table 4
Simulated counting rates for uniform (ρ_u) and non-uniform (ρ_{nu}) source distributions, correction factors (CF_{MCNP}) and probe corrected efficiencies (ε_{MCNP}).

Nuclide Source	ρ_u (cps)	ρ_{nu} (cps)	CF_{MCNP}	ε_{MCNP} (%)
^{14}C	9.61	8.15	1.179 ±0.003	23.8 ±0.7
^{99}Tc	22.73	23.19	0.980 ±0.003	37.2 ±1.1
^{36}Cl	34.45	32.07	1.074 ±0.003	52.3 ±1.4
^{90}Sr	49.79	50.44	0.987 ±0.003	55.7 ±1.5

3.2. Calibration

Table 3 shows the experimental net counting rates (ρ_c), that were obtained using the LARS presented in Table 1, the source emission rate under the probe sensitive area (SER) and the instrument efficiency estimates (ε) calculated by applying equation (1), i.e., without correction.

Table 5
Effective surface emission rates (SER_{eff}) and the corrected instrument efficiency estimates (ε_{NPL}).

Nuclide / Source	SER_{eff} ($\beta.s^{-1}$)	ε_{NPL} (%)
^{14}C	35.5 ±1.1	23.8 ±0.9
^{99}Tc	60.2 ±1.7	37.2 ±1.1
^{36}Cl	61.9 ±1.6	52.2 ±1.5
^{90}Sr	89.0 ±2.4	55.6 ±1.5

Table 6
Correction factors comparison.

Nuclide / Source	CF_{MCNP}	CF_{NPL}
^{14}C	1.179 ±0.003	1.18 ±0.05
^{99}Tc	0.980 ±0.003	0.98 ±0.04
^{36}Cl	1.074 ±0.003	1.07 ±0.04
^{90}Sr	0.987 ±0.003	0.99 ±0.04

3.3. Correction factor - simulation method

Table 4 presents the simulated counting rates values for surface contamination monitor probe, for each of the sources mentioned in Table 1, for two representations of intensity distributions: uniform and non-uniform. The numerical uncertainties of the simulation results were always below ± 0.2%. It is also shown in this table the correction factor values (CF_{MCNP}) and the corrected efficiencies of the instrument (ε_{MCNP}).

3.4. NPL method

The method for large-area reference source uniformity correction proposed by NPL is based on the evaluation of the effective emission rate of the source area under which the radiation monitor probe is positioned. Table 5 presents the effective surface emission rate (SER_{eff}) of the area under the input window of the probe and the corrected instrument efficiency estimate (ε_{NPL}) by applying the procedures proposed by NPL for the sources used in this work.

3.5. Differences between simulation and NPL methods

Both correction procedures aim to correct the calibration efficiency values attributed to the instrument. In the case of the numerical method presented by NPL the correction is applied to the source emission rate values as can be observed by equation (7). However, the correction method proposed in this work applies to the counting rate registered by the instrument probe (equations (3)–(5)). Both methods take into account the LARS uniformity mapping. As the ultimate objective of both methods is to correct the instrument efficiency value, correcting either the source emission rate or the instrument counting rate should provide the same final result. Using the numerical method of NPL, it is possible to adopt a correction factor (CF_{NPL}) that can be applied directly to the uncorrected instrument efficiency, instead of correcting the flow value of the large-area reference source. This new factor is obtained according to equation (9).

$$CF_{NPL} = \frac{SER}{SER_{eff}} \tag{9}$$

Table 6 presents the correction factors driven from simulation method presented in this work and from the NPL method, so to allow a comparison between the correction factors values obtained from these methods.

With these correction factors (CF_{MCNP} and CF_{NPL}), it is possible to calculate the corrected instrument efficiency (ε_{MCNP} and ε_{NPL}) by simply multiplying the estimated value of the uncorrected instrument efficiency (ρ) by the correction factor associated to a radionuclide, as it is shown by equations (10) and (11).

$$\varepsilon_{MCNP} = \varepsilon \times CF_{MCNP} \tag{10}$$

$$\varepsilon_{NPL} = \varepsilon \times CF_{NPL} \tag{11}$$

4. Discussion

The used ^{99}Tc and ^{90}Sr LARS, the ones that meet the minimum 90% uniformity value, have shown to lead monitor probe efficiency biased values that are overestimated by 2% in the worst case. The ^{14}C and ^{36}Cl, the ones not complying with the ISO 8769 uniformity criterion have led to monitor efficiency values biased from the expected value by as much as 17%. It is noteworthy to stress that the biased values found are specific for the system configuration taken into account, which includes the specific LARS and detector taken into account and their relative arrangement.

A source uniformity correction methodology based on Monte Carlo simulations has been developed to get more accurate instrument efficiency estimates. Simulations surface contamination monitors calibration setup were carried out to estimate their counting rates for different surface source distributions. Data presented in Fig. 3, provides the confidence on the simulated results that stands as a key point of the methodology. Simulations were thereafter used to quantify the expected differences it would be observed in detector counting rates between the use of real and the ideal surface source distributions. Correction factors were driven from the simulated counting rate ratios between the uniform and real surface source distribution. No restrictions were applied to the uniformity value. The methodology provides a correction factor that shall be applied to the experimental efficiency removing the eventual bias it would be inferred by the use of a real LARS rather than a 100% uniform LARS.

The comparison between corrected instrument efficiency values obtained with the simulation method presented in this work (Table 4) and by applying the NPL method (Table 5) show equivalent results for all 4 sources used along this work. This is even true for sources, which present uniformity values below the 90% minimum reference value. These sources would not stand along the eligible sources to apply the NPL uniformity correction methodology.

Although the correction factors were obtained by different ways, they present good compatibility with each other, which can be easily seen by the correction factor values presented in Table 6.

5. Conclusions

We have proposed a methodology to study the effect of surface source uniformity distribution on detector efficiency estimate procedures. The methodology, based on MCNP5 simulations, was experimentally validated and compared to the NPL uniformity correction procedure. Simulated results for the four LARS used in this work have shown differences in the instrument efficiency values attributed to the Thermo radiation monitor model FH40GX by adopting different reference source uniformity criteria, i.e., with uniformity equal to 100% and real non-uniform distribution (uniformity less than 100%). The lesser the source uniformity the larger were the differences found. Corrections were no larger than 2% for the sources attaining the ISO 8769 uniformity criteria, while it has reached 17% for the 14C LARS with a 50.2% uniformity value.

Acknowledgments

Authors would like to acknowledge Fundação de Amparo à Pesquisa

do Estado de São Paulo (FAPESP, 2008/57863-2) and Conselho Nacional de Desenvolvimento Científico e Tecnológico (CNPq), for partially supporting this work.

References

Choi, C.H., Jung, S., Choi, K., Son, K.-J., Lee, J.S., Ye, S.-J., 2016. Radioactivity determination of sealed pure beta-sources by surface dose measurements and Monte Carlo simulations. Nucl. Instrum. Methods Phys. Res. Sect. A Accel. Spectrom. Detect. Assoc. Equip. 816, 87–95. https://doi.org/10.1016/j.nima.2016.01.085.

Farsoni, A.T., Hamby, D.M., 2005. MCNP analysis of a multilayer phoswich detector for β-particle dosimetry and spectroscopy. Nucl. Instrum. Methods Phys. Res. Sect. A Accel. Spectrom. Detect. Assoc. Equip. 555 (1–2), 225–230. https://doi.org/10.1016/j.nima.2005.09.025.

Grujić, S., Đorđević, I., Milošević, M., Kozmidis-Luburić, U., 2013. Monte Carlo simulation of GM probe and NaI detector efficiency for surface activity measurements. Radiat. Meas. 58, 45–51. https://doi.org/10.1016/j.radmeas.2013.08.002.

ISO, 7503-3, 2016. Measurement of radioactivity — Measurement and evaluation of surface contamination — Part 3: Apparatus calibration. International Organization for Standardization, Geneva.

ISO, 8769, 2016. Reference sources — Calibration of surface contamination monitors – Alpha-, beta- and photon emitters. International Organization for Standardization, Geneva.

Lee, C., PH, B., 2014. Good Practice Guide No. 14 (Issue 2). National Physical Laboratory, United Kingdom.

Ohshiro, M., Shiina, T., Yamada, T., 2016. Uniformity measurement of wide area reference sources for beta emitters. Appl. Radiat. Isot. 109, 397–401. https://doi.org/10.1016/j.apradiso.2015.12.015.

X-5 Monte Carlo Team,i, 2003. MCNP - Version 5, Vol. I: Overview and Theory. LA-UR-03-1987.

Radar the decay data, http://www.doseinfo-radar.com/RADARDecay.html, accessed: 2019-08-26.

Ródenas, J., Burgos, M C, Zarza, I., Gallardo, S., 2005. Simulation of germanium detector calibration using the Monte Carlo method: comparison between point and surface source models. Radiat. Protect. Dosim. 116 (1–4), 55–58. https://doi.org/10.1093/rpd/nci111.

Silva Junior, I.A., Xavier, M., Siqueira, P.T.D., Potiens, M.P.A., et al., 2014. Avaliação da homogeneidade das fontes planas de referência utilizadas na calibração de monitores de contaminação de superfície, RADIO 2014 - International Joint Conference.

Vivolo, V., Potiens, M.P.A., 2010. Evaluation of the planar sources surface homogeneity used to instruments calibration. Appl. Radiat. Isot. 68 (4–5), 605–606. https://doi.org/10.1016/j.apradiso.2009.09.017.